

OFDM Receiver Performance Analysis with Measured Channel Model for Power Line Communication

Yonghwa Kim, Hui Myong Oh*¹ and Seong Cheol Kim
Institute of New Media and Communications,
School of Electrical Engineering and Computer Science,
Seoul National University, Seoul, Korea
*¹ Korea Electrotechnology Research Institute

Abstract

This paper reports the results of wideband channel measurements conducted on in house outlets. Two kinds of channel measurements were performed: impulse response measurements and noise signal measurements. In measure based channel model, preamble assisted orthogonal frequency-division multiplexing access (OFDM) receiver scheme is proposed for differential phase shift keying (DPSK) and quadrature amplitude modulation (QAM). Timing synchronization and channel estimation is performed using the preamble. We provide numerical results to illustrate the performance of OFDM receiver in measure based channel model.

Keywords: Power Line Communication, channel measurement, OFDM, channel coding, synchronization

1 INTRODUCTION

In-house power line has recently been considered as an alternative medium for high speeds data transmission in applications such as home networking and Internet access. Power line communication takes the advantage of use in everyplace at home without additional network line. However, power line channel is the time-and-frequency variant and exhibits remarkable difference between locations, according to its network topology, the types of wire lines [1]. So the study of channel is very useful in the design of wideband power line communication systems. In this paper, to obtain channel impulse response, measurements were carried out using the pseudo-random noise (PN) correlation method. Noise signal strengths at swept frequencies were measured at the same environment as impulse response measurements.

The orthogonal frequency-division multiplexing (OFDM) has recently received considerable attention for its robustness against frequency selective multi-path channel and impulsive noise [2]. So the PLC standard by the HomePlug [3] uses OFDM access technology for reliable power line communication. As shown fig. 1, the OFDM access technology is based on the transmission of data packets, each data packet consists of a preamble and a data carrying part. The preamble consists of 7.5 known OFDM symbols of length $N_s = 256$ and are used for auto gain control (AGC), carrier frequency offset correction, synchronization and channel estimation. The 7.5 known OFDM symbols composed of 6 SYNCP signals and 1.5 SYNCM signals where SYNCM is the opposite sign to SYNCP. The data carrying part consists of a variable number of OFDM symbols. Each data OFDM symbol has the length $N_d = N_s + N_{cp}$, cyclic prefix length

$N_{cp} = 172$. The HomePlug 1.0 specification can provide data rates up to 14Mb/s. It uses concatenated codes, convolution codes as an inner code and Reed-Solomon (RS) codes as an outer code.

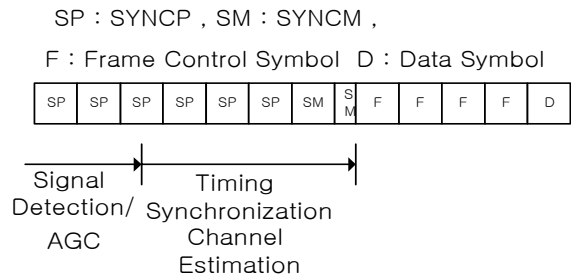


Fig. 1 Frame Structure for HomePlug 1.0

The focus of our paper is on the impact of multi-path dispersion and colored noise on the performance of the OFDM receiver by HomePlug 1.0 specification. The multi-path dispersion affects the synchronization timing error. The synchronization timing error of the proposed algorithm for preamble is examined in comparison papers for wireless LAN systems [4], [5]. The impact of colored noise, different from conventional AWGN, is on the channel estimation and data demodulation. So we examine performance of a preamble assisted OFDM receiver in measure based channels for DPSK and QAM, an attractive modulation due to its spectral efficiency.

The organization of the rest of this paper is as follows. The channel model based on channel measurement is described in section 2. In section 3, we consider the OFDM systems for measured channel model. In section 4, the synchronization

algorithm for preamble and data demodulation is described and in section 5, numerical results are provided to evaluate the performance of the proposed algorithms in measured all channels. Finally, conclusions are drawn in section 6.

2 Channel Model

2.1 Multi-path Channel Model

Power line channel at home has the time-and-frequency variant because it doesn't design for communication. So reliable power line communication system, to obtain impulse response results is necessary. The measurements were carried out using the pseudo-noise (PN) correlation method to obtain channel impulse response [6]. Fig. 2 shows the measurements system to obtain wideband channel impulse response using PN correlation method.

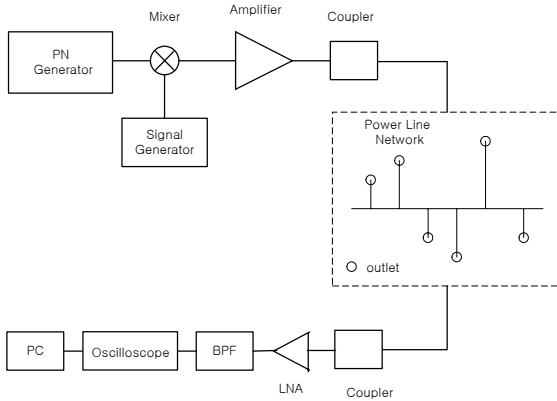


Fig. 2 Channel Sounding System

50 power delay profiles (PDPs) were taken for 86 seconds. The statistical properties of amplitudes of each path are also obtained from measured impulse responses. Let

$$h(\tau; t) = \sum_{l=1}^{N_p} \alpha_l(t) \cdot \delta(\tau - d_l(t))$$
 be a multi-path channel model number, α_l is the channel fading coefficient of l th path and d_l is the delay of l th path where l represents path, N_p is the number of multi-path. For multi-path channel model, the characteristic of $\alpha_l(t)$ is necessary. So the fading coefficient

of each path represents the cumulative distribution functions (CDFs) by measured impulse response results and CDFs were found to fit a Rician distribution [7]. For power line modem performance analysis, we give an example of channel model such as Table 1 where K is the Rician factor. Channel dispersion of in-house power line as Table 1 shows $d_{N_p} \leq N_{cp}$ and a mean power of $\sigma_l^2 = E[|\alpha_l|^2]$ for $l = 1, \dots, L$ is such that $\sum_{l=1}^L \sigma_l^2 = 1$. The channel is fixed during the transmission of one packet but independent from one

packet to another.

2.2 Noise Model

For wireless communication, noise model is assumed AWGN. However, many different noises exist in power line communication network. So noise of power line channel is assumed colored noise [8], [9]. After we measured narrowband noise of power line channel from 1 to 30MHz by spectrum analyzer, the method of cumulative probability distribution (CPD) is used for power line colored noise model [10].

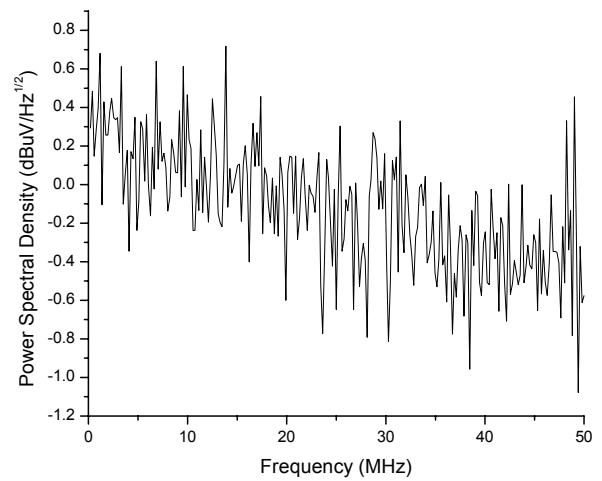


Fig. 3 Power Spectral Density of Colored noise

Let colored noise $n_{cl}(t)$ and its spectral density function $N(f)$, respectively. Fig. 3 shows a normalized $N(f)$ of colored noise by computer simulation. Let $2\sigma_n^2 = E[|n_{cl}(t)|^2] = N(f) \cdot W = N_{cl}$ be the variance of colored noise where bandwidth W is 50MHz and E_b / N_{cl} be the bit energy to noise variance. The power spectral density of colored noise $N(f)$ is fixed during the transmission of one packet but independent from one packet to another. Also $n_{cl}(t)$ is independent from one OFDM symbol to another.

3 OFDM SYSTEM IN POWER LINE COMMUNICATION

Due to its effectiveness in frequency selective channels and colored noise, OFDM system is well-suited for communication over power lines. Let d be data bits and c be encoded bits. Concatenated codes are used for channel codes, convolutional codes as inner codes and Reed Solomon codes as outer codes [11]. The encoded bits are passed through a block channel interleaver. Let X which belong to $A = \{\alpha_1, \alpha_2, \dots, \alpha_{2^M}\}$ be modulated symbols for DBPSK ($M = 1$), DQPSK ($M = 2$) or

Table 1. Multi-path model for numerical analysis

4-path model				8-path model							
Path	α	d (us)	K	Path	α	d (us)	K	Path	α	d (us)	K
1	11.13	0	50	1	19.46	0	50	5	1.62	0.58	10
2	1.18	0.2	30	2	6.85	0.18	30	6	1.82	0.72	5
3	3.43	0.34	10	3	4.03	0.32	10	7	1.75	0.88	5
4	0.8	0.58	5	4	2.46	0.46	10	8	0.97	1.18	5

16 QAM ($M = 4$). The symbols are then split into groups modulated onto N_s symbols and each symbol is modulated onto one of N_s orthogonal sub-carriers. The transmitted signal $x(t)$ is obtained by IFFT such that

$$x(t) = \frac{1}{N_s} \sum_{k=0}^{N_s-1} X[k] e^{j2\pi kt/N_s} \quad (1)$$

where $X[k]$ is the data symbol X of k^{th} sub-carrier frequency. A cyclic prefix of length N_{cp} samples is then added to form a cyclically extended OFDM symbol. Then, the received signal $r(t)$ with measured channel model can be written as

$$r(t) = h(\tau; t) \otimes x(t) + n_{cl}(t) \quad (2)$$

where $h(\tau; t)$ and $n_{cl}(t)$ are defined on section 2 and \otimes denotes convolution.

Prior to demodulation in an OFDM receiver, signal detection, AGC, timing synchronization and channel estimation are executed at preamble of each packet. As shown Fig. 1, signal detection and AGC are completed at some arbitrarily point in time relative to the start of the preamble. Timing synchronization algorithm for preamble over power lines represents in section 4. After timing synchronization, the receiver removes the guard interval and feeds the remaining N_s samples are fed to the FFT processor for demodulation.

During data demodulation, the timing error of preamble synchronization algorithm is tolerable as long as the receiver FFT window starts within the guard interval of the first arriving path that is not affected by the previous symbol. In such a *lock-in* region, the orthogonality among the sub-carriers is preserved [12]. So the *lock-in* probability can be achieved by

$$P_{lock-in} = \frac{N_{lock-in}}{N_{Frame}} \quad (3)$$

where $N_{lock-in}$ is the number of frames whose timing synchronization starts in the *lock-in* region and N_{frame} is the transmitted frame number.

If timing synchronization performs within *lock-in* region, the output of FFT processor for demodulation can be written as

$$R[k] = H[k] \cdot X[k] + N_{cl}[k] \quad (4)$$

where $H[k] = \sum_{l=1}^{N_p} \alpha_l(k) \cdot e^{-j2\pi k d_l(k)/N_s}$ is the frequency response at the k^{th} sub-carrier; $Y[k]$ and $X[k]$ are the received signal and the transmitted symbol at the k^{th} sub-carrier, respectively; $N_{cl}[k]$ is the colored noise, which is the FFT output of $n_{cl}(t)$.

4 OFDM receiver

Assuming signal detection and AGC is completed at the receiver, time synchronization algorithm finds the start point of each SYNC signal. For time synchronization, the received signal samples correlates with the known OFDM symbol SYNCP. The correlation equation is given by

$$R_n = \sum_{m=1}^{N_s} r(n-256+m) PS^*(m) \quad (5)$$

where PS is the SYNCP signal and R_n is the output of correlation process. We find the maximum $|R_n|^2$ of N_s outputs and then maximum value compare with the next maximum $|R_n|^2$ of N_s outputs. We update the maximum value $\mu_i = \max_{n < i} |R_n|^2$ and the position n_i of maximum value by this process. If $n - n_i$ is a multiple of N_s and satisfy equation (6), the correlation process is stopped.

$$0.5\mu_i > |R_n|^2 \quad (6)$$

The end position of preamble and the number of SYNC declare $\hat{N}_{frame} = n - N_s + 128$ and $\hat{N} = (\hat{N}_{frame} - 128) / N_s$. For timing synchronization algorithm analysis, the MSE_{sqr} is defined by

$$MSE_{sqr} = \sqrt{\left(E \left[\left[N_{frame} - \hat{N}_{frame} \right]^2 \right] \right)} \quad (7)$$

where N_{frame} is the exact end position of preamble.

After timing synchronization algorithm is completed, the channel parameters for the demodulation of data bits can be estimated by

$$\hat{H}(k) = \frac{\frac{1}{\hat{N}} \cdot \sum_{n=0}^{\hat{N}-1} \left(\frac{1}{\sqrt{N_s}} \sum_{i=\hat{N}_{preamble}-128-N_s(n+1)}^{\hat{N}_{preamble}-128-N_s n} x(i) e^{j2\pi k / N_s} \right)}{P(k)} \quad (8)$$

where $P(k)$ is the pilot symbol of k^{th} sub-carrier frequency at preamble.

For data bits demodulation for DBPSK and DQPSK in HomePlug 1.0, the end position of preamble only used to the FFT processor. After FFT processor, frame control bits and data bits were detected by coherent demodulation and by differentially demodulation, respectively. Information bits were obtained for convolutional codes by hard-decision based Viterbi algorithm [13] and for RS codes by Euclidean methods [14].

For QAM-OFDM system, a rate 1/2 convolutional code of constraint length 7 was used. The generator polynomials were 133 and 171 in octal and the block length was 1680. Preamble used the same structure by HomePlug 1.0. For soft-decision decoding, the log-likelihood ratio $\Lambda(c)$ (LLR) of the coded bits c is obtained by

$$\Lambda(c) = \frac{1}{\sigma_{n_{cl}}^2} \left(\min_{X^- \in \{X:c=-1\}} |R - \hat{H}X^-|^2 - \min_{X^+ \in \{X:c=+1\}} |R - \hat{H}X^+|^2 \right) \quad (9)$$

where R is the output of FFT process and \hat{H} is the channel estimate. Viterbi algorithm performs using the LLR [15].

5 Numerical Results

Simulation results exhibit the effectiveness of the timing synchronization algorithm in colored noise channel and in measured multi-path channel with colored noise. Fig. 4 shows the *lock-in* probability. Horizontal axes indicate a

signal-to-noise ratio (SNR) ranging from 0 to 7 dB in Fig.4. We can see that *lock-in* probability at an SNR of 0 dB is about 0.95 in colored noise channel, about 0.86 in 4-path channel and 0.73 in 8-path channel. The *lock-in* probability exceeds 0.97 when SNR is more than 5.0 dB in all channel models.

Fig. 5 shows the BER performance for DBPSK in colored noise channel and multi-path channel with colored noise. We observe that BER in colored noise channel performs better than BER in multi-path channel with colored noise about 4 dB at a BER around $5 \cdot 10^{-3}$. We observe that there exists performance degradation in multi-path channel model and convergence at a BER around $5 \cdot 10^{-3}$ in 8-path model.

As shown in Fig. 6, MSE_{sqr} value in colored noise is 0 when SNR is more than 4 dB. In 4-path channel of Fig. 6, MSE_{sqr} values lie in the range from 8 to 200. In addition, the MSE_{sqr} values lie in the range from 28 to 314 in 8-path channel of Fig.6. But, if timing synchronization performs in *lock-in* region, MSE_{sqr} is 0 in all channel models. This indicates that timing error exists for data demodulation in multi-path channel model when timing synchronization can't start in the *lock-in* region.

Horizontal axes indicate E_b / N_{cl} ranging from 0 to 5 dB in Fig. 7. In fig. 7, assuming timing error doesn't exist, we observe that the BER in colored noise channel for 16-QAM performs better than BER in multi-path channel with colored noise for 16-QAM about 3 dB and about 0.5 dB for DQPSK at a BER around 10^{-3} . Also, the BER for 16-QAM OFDM converges $5 \cdot 10^{-4}$ in all channels.

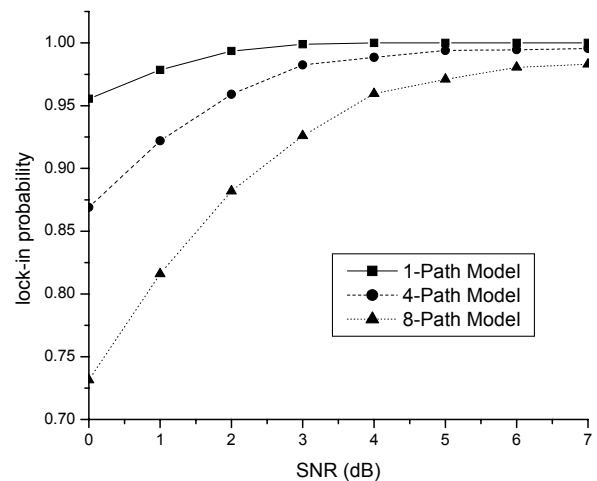


Fig. 4 *lock-in* probability

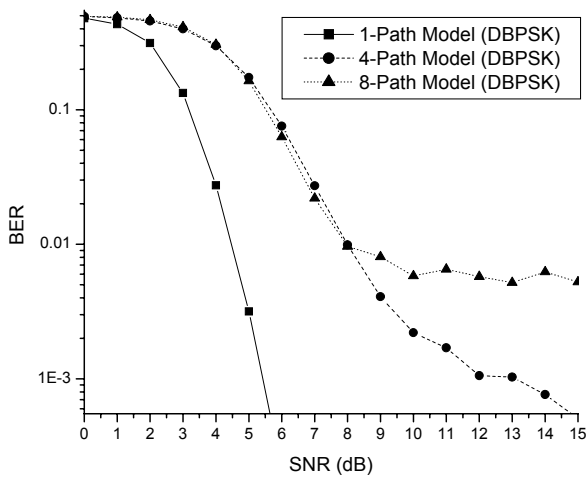
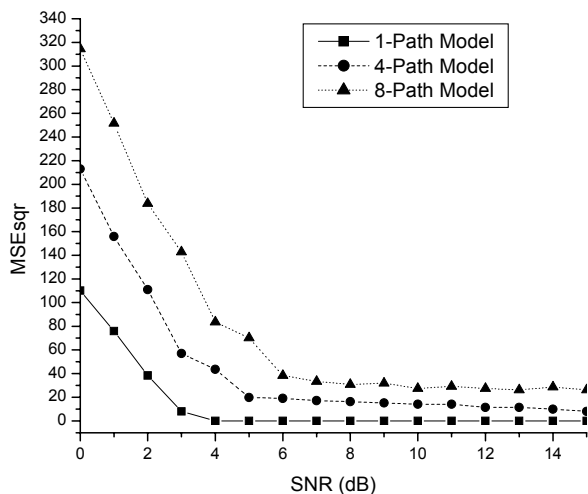


Fig. 5 BER for DBPSK

Fig. 6 MSE_{sqr} for timing synchronization

6 Conclusions

In this paper, the communication channel properties of in-house power line are characterized through impulse response measurements and noise measurements. Also, the performance of OFDM receiver in measure based multi-path channel over power lines is analyzed. In OFDM receiver, timing synchronization algorithm for HomePlug 1.0 preamble structure has been shown to be robust more than 3.0 dB in all channels. We observed the BER for DBPSK with synchronization timing error by timing synchronization in all measured channels and the BER for 16-QAM without synchronization timing error. The BER for DPBSK at $5 \cdot 10^{-3}$ performance degradation of SNR 3 dB in multi-path channels

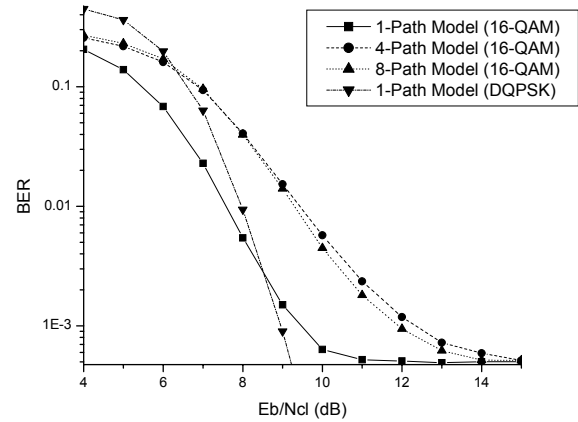


Fig. 7 BER for 16-QAM

and the BER in 8-path model converges $5 \cdot 10^{-3}$. The BER for 16-QAM OFDM converges $5 \cdot 10^{-4}$ in all channels.

Acknowledgement

This research was supported by University IT Research Center Project

REFERENCES

- [1] Y.-J. Lin, H. A. Latchman, R. E. Newman, S. Katar, "A comparative Performance Study of Wireless and Power Line Networks", *IEEE Comm. Mag.* vol. 41, issue: 4, pp. 54-63, April 2003.
- [2] Nguimbis J., Shijie Cheng, Youbing Zhang, Haibo He, Lan Xiong, "On the design of a broadband low impedance load mitigating coupling unit for efficiency OFDM signal power transfer maximization through the PLC network", *Proc of PowerCon 2002*, vol. 2, Oct. 13-17, 2002, pp. 1316-1321.
- [3] HomePlug, <http://www.homeplug.com/>
- [4] S. Chang, B. Kelley, "Time synchronisation for OFDM-based WLAN systems", *Electronics Letters*, vol. 39, pp. 1024-1026, June 2003.
- [5] K. W. Yip, T. S. Ng, Y. C. Wu, "Impacts of Multipath Fading on the Timing Synchronization of IEEE 802.11a Wireless LANs", *Proc of ICC 2002*, vol. 1, 28 April-2 May, 2002, pp. 517-521.
- [6] D. C. Cox, "Delay doppler characteristics of multipath propagation at 910MHz in a suburban mobile radio environment", *IEEE Trans. Antennas Propagat.*, vol. AP-20, no.5, pp. 625-635, Sep. 1972.
- [7] Y. H. Kim, H. H. Song, J. H. Lee, S. C. Kim, "Wideband Channel Measurements and Modeling for In-House Power Line Communication", *Proc of ISPLC2002*, March 27-29, 2002, pp 189 – 193.
- [8] F. J. Canete, J. A. Cortes, L. Diez, J. T. Entrambasaguas, "Modeling and Evaluation of the Indoor Power Line Transmission Medium", *IEEE Comm. Mag.* vol. 41, issue: 4,

pp. 41-47, April 2003

- [9] H. C. Ferreira, H. M. Grove, O.Hooijen, and A. J. Han Vinck, " Power line communications : an overview", Proc of AFRICON 4th, vol. 2, Sept. 27-29, 1996, pp. 558-563.
- [10] L. T. Tang, P. L. So, E. Gunawan, Y. L. Guan, S. Chen, T. T. Lie, "Characterization and modeling of in-building power lines for high-speed data transmission," IEEE Trans. Power Delivery, vol. 18, pp. 69-77, Jan. 2003.
- [11] HomePlug Powerline Appliance 1.0.1. Specification, 2001.
- [12] D. Lee, K. Cheun, "Coarse Symbol Synchronization Algorithms for OFDM systems in Multipath Channels", Com. Letters, vol. 6, issue: 10, pp. 446-448, Oct. 2002.
- [13] R. Blahut, Algebraic Codes for Data Transmission, Cambridge University Press, 2003.
- [14] S. B. Wicker, and V. K. Bhargava, Reed-Solomon Codes and Their Applications. New Jersey, 1983
- [15] T. May, H. Rohling, V. Engels, "Performance analysis of Viterbi decoding for 64-DAPSK and 64-QAM modulated OFDM signals", IEEE Trans. Comm., vol. 46, issue : 2, pp. 182-190, Feb. 1998

Yonghwa Kim received his BS and MS degrees from Seoul National University in 2001 and in 2003, respectively. He is also pursuing his Ph. D. degree at the Seoul National University, Korea. His research interests are in channel estimation algorithms and performance analysis of wireless communication systems such as CDMA, OFDM and MIMO systems, and power line communication.

Hui Myong Oh received his BS and MS degrees from Yonsei University in 1998 and in 2000, respectively. He has been a research staff at the Korea Electrotechnology Research Institute. He is also pursuing his Ph. D. degree at the Yonsei University, Korea. His research interests are in digital communication systems and power line communication, and OFDM.

Seong Cheol Kim received his BS and MS degrees from Seoul National University and Ph.D. degree from Polytechnic University, respectively. He has been a research staff at the Center for Advanced Telecommunication Technologies in Polytechnic University. He also worked for the R&D department of Symbol Technologies, Inc.

Since 1995, he had been with Wireless communications Systems Engineering Department at AT&T Bell Laboratories, Holmdel, NJ until he joined Seoul National University as a faculty member, March 1999.

He is now an associate professor at School of

Electrical Engineering of Seoul National University. His research interests cover the characterization and modeling of radio wave propagation for wireless communications systems, wireless channel modeling, wireless systems engineering, channel estimation algorithms and performance analysis of wireless communication systems such as CDMA, OFDM and MIMO systems. He has also studied the power line communication focusing on channel modeling and performance analysis of modem algorithm.